A Microfluidic Spherical Helix Module Using Liquid Metal and Additive Manufacturing for Drug Delivery Applications

Yangyang Guan [#1], Shicong Wang[$2], Manos M. Tentzeris[*3], Yuanan Liu[#4]

[#]Beijing Key Laboratory of Work Safety Intelligent Monitoring,
Beijing University of Posts and Telecommunications, China

[$]Key Laboratory of Embedded System and Service Computing of the Ministry of Education,
Tongji University, China

[*]Agile Technologies for High-performance Electromagnetic Novel Applications,
Georgia Institute of Technology, USA

[1]ivory_tower@outlook.com, [2]swang719@gatech.edu, [3]etentze@ece.gatech.edu, [4]yuliu@bupt.edu.cn

***Abstract*—In this paper, a spherical helix module based on 3D printing and microfluidic technologies was fabricated, tested and applied to drug delivery applications. A liquid metal alloy is introduced to enhance the sensitivity of the complex and drug-/liquid-reconfigurable helix topology. Moreover, the influence of the dimensions of the hemisphere inscribed by the helical turns on the resonant frequency of the structure is researched. The microfluidic channels with 1 mm radius are shaped in the form of double semispherical helix using a Form-2 3D printer. To fulfill effectively the liquid metal (LM) injection, movement and recycle for reuse, a syringe pump is integrated to flexibly control the flow of the fluid. Besides, the proof-of-concept prototype achieves excellent radiation gain and impedance matching. The realized sensitivity is 0.96 mL/GHz and 0.33 mL/GHz corresponding with the frequency shift from 2.28 to 2.01 GHz and 2.01 to 1.65 GHz.**

***Keywords*—additive manufacturing, microfluidic, liquid metal, spherical helix module, drug dosage monitoring.**

I. Introduction

Due to various applications like chemical storage, drug level monitoring and fuel transportation, liquid level detection plays an increasingly important role in our daily life. Due to the corrosiveness and the danger of most acidic or alkaline chemical liquids of high concentration, monitoring the liquid level is a challenging task eliminating the possibility of direct contact or direct exposure in various work environments. Besides, in the process of infusion, monitoring the change of the liquid medicine level can effectively avoid the dangerous situation of "blood return" for the patient. Considering the above crucial requirements, it's essential for researchers to pay attention towards effective tetherless liquid delivery monitoring techniques.

In the past few years, many kinds of liquid level sensing techniques have been reported, including electrical and optical technologies. Numerous optical fiber based sensors have been designed to monitor the liquid level. In [1], an all-optical-fiber sensor is proposed for the continuous measurements of liquid levels. A liquid level sensor based on plastic optical fibers (POFs) is described in [2]. For wireless monitoring applications, radiofrequency identification (RFID) sensors have been introduced in [3]. In this paper, we propose a novel spherical helix antenna based on 3D printing and microfluidic technologies for wireless liquid level monitoring. The monitoring function is activated when the drug level reaches just below the top outlet of the module. And the length of the radiation arm of the antenna decreases simultaneously with the level of the monitored liquid. Then this process can be followed and recognized with the performances of the designed antenna.

The combination of additive manufacturing techniques (AMTs) with microfluidics feature low cost, high repeatability, complex 3D structure fabrication and environmental friendliness [4]. Due to the difficult fabrication of the proposed spherical helix topology, 3D printing is adopted for the manufacturing of two hollow semispherical support structures along with helical microfluidic channels wrapped around them in helical configurations. Using a Form-2 3D printer, the proposed monitoring module in the shape of double semispherical helix was entirely printed without any need for assembly.

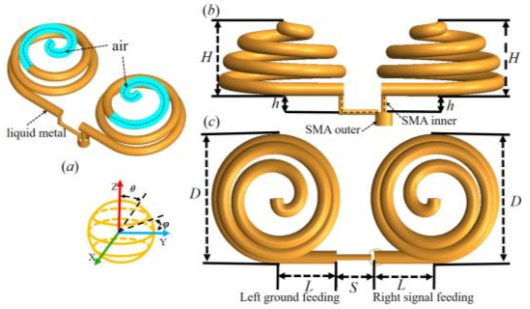

Fig. 1. The topology of the proposed helix antenna. (a) 3-D view. (b) Front view. (c) Top view. This antenna is directly excited by two feeding cylinders with the length *L* and a gap *S* between the two feeding lines. The height *H* and the diameter *D* of the hemi-sphere support are marked in the picture.

Finally, the presented module with three spherical helix turns per semispherical branch and 0.82 mL capacity is measured at 3 turns state, 2 turns state and 1 turn state filled with LM. For each measurement at a static state, a small cylindrical cap shaped like a "hat" is utilized to stabilize the level of the LM. The proof-of-concept prototype achieves good radiation gain and return loss (S_{11}) of -7.5 dB, -16.2 dB

and -15.5 dB at the resonant frequencies of 1.65 GHz, 2.01 GHz and 2.28 GHz, respectively.

II. Spherical Helix Module

A. Structure of Module

The proposed 3D spherical helix module is shown in Fig. 1. The topology comprises of two symmetrical arms and two feeding cylinders. The feeding cylinders with the length L (9 mm) are connected to a SubMiniature version A (SMA) connector. Shown in Fig. 1, the right cylinder is connected with the inner layer of a SMA extension cable to feed the input signal and the left cylinder is connected with the outer layer of the SMA extension cable as a ground. The gap (S) between the two feeding lines is 5.6 mm. In this design, the spherical helix microfluidic channel is wrapped on a hollow hemi-sphere. The diameter (D) of the hemi-sphere is 17.6 mm and H is half of the diameter. The height h is 3.4 mm for the inner connection. The two semispherical microfluidic channel structures along with the contained LM act as the radiation arms of an antenna.

B. Theory and Simulation

According to the planar spiral antenna shown in [5], the total spiral length can be easily approximated. For the designed spherical helix structure, the two same semispherical helix models both are equal pitch and can be described correlating θ and φ as shown in equation (1). The equations of a spherical surface in Cartesian coordinates system is presented as equation (2), where H is the radius of the (semi) spherical support structure and A is the number of the helix turns.

$$\theta = cos^{-1}\left(\frac{\varphi}{A\pi} - 1\right) \tag{1}$$

$$\begin{cases} x = Hsin\theta cos\varphi \\ y = Hsin\theta sin\varphi \\ z = Hcos\theta \end{cases} \tag{2}$$

$$\begin{cases} x = H\sqrt{1-\left(\frac{\varphi}{A\pi}-1\right)^2}\, cos\varphi \\ y = H\sqrt{1-\left(\frac{\varphi}{A\pi}-1\right)^2}\, sin\varphi \\ z = H(\frac{\varphi}{A\pi}-1) \end{cases} \tag{3}$$

By substituting equation (1) into equation (2), the equation for a spherical helix in Cartesian coordinates system is acquired in equation (3). In this paper, φ takes the values between $A\pi$ and $2A\pi$ for hemi-sphere. The two semispherical helices are described by the same equations. Each helix equally divides the radius in the axial direction into A parts. The simulation software of High Frequency Structure Simulator (HFSS) is used to create a model using equation (3). For simplicity purposes, a perfect conductor model was utilized for the LM. Here, we assume that the material of the channel has a minimal influence on the resonant frequency. Thus, the dielectric materials of the microfluidic channels and the hemispherical support structure actually printed with "clear" material are not considered in the simulation. As shown in Fig. 2, the relationship between the resonant frequency and the radius H is displayed. The resonant frequency shifts down from 2.7 GHz to 1.87 GHz when the radius H increases from 8 mm to 12 mm.

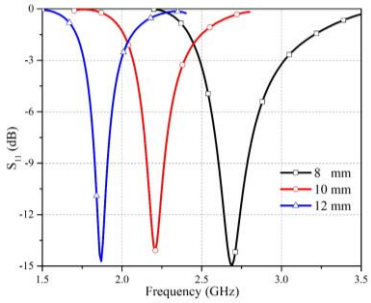

Fig. 2. The relationship between the resonant frequency and the radius H.

Considering the minimum printing size and aiming for the largest possible capacity, the radius H is finally determined as 8.8 mm and the radius of the channel is 1 mm. The suggested wall thickness for a hollow cylindrical microfluidic channel is 0.4 mm. Due to the equal pitch semispherical helical structure, the radius H will be equally divided into A parts. The minimum height l_{min} of each microfluidic part/section is the sum of two wall thickness of the channel and the diameter of the channel (l_{min}=2.8mm). Thus, once the radius H was selected as 8.8mm, the maximum turns A_{max} will be limited to 3. The capacity of the two semispherical helical channels finally reaches up to 0.82 mL. Here, the volume of the filled LM inside the two semispherical branches corresponding with the selected resonant frequency are tabulated in Table 1.

Table 1. The resonant frequency varies with the volume of the filled LM (simulation).

A	***V* (mL)**	***f* (GHz)**
1.0	0.44	2.24
2.0	0.70	1.96
3.0	0.82	1.71

Note: V-volume of the filled LM inside the channels; f-resonant frequency;

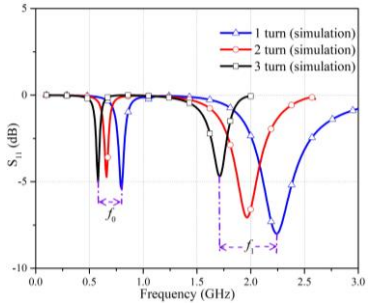

Fig. 3. The simulated resonant frequencies shift down with increase of the number of the filled turns with LM.

As described in Fig. 3, the dominant mode frequency f_0 and the second-order mode frequency f_1 both shift monotonically down with the value of A (numbers of turns of every branch that are fully filled with LM) increases from 1 to 3. For increased sensitivity, the resonant frequencies utilized for the monitoring of the drug level are selected to correspond to the second-order mode. The marking frequencies are

selected at the second-order mode of f_1, where the frequency for 3 turns state is 1.71 GHz, the frequency for 2 turns state is 1.96 GHz and the frequency for 1 turn state is 2.24 GHz.

III. Fabrication and Experiments

A. 3D Printing

Due to the challenges with the fabrication of the spherical structure and helix microfluidic channels with small size and complex 3D topology, the conventional fabrication technologies were hard to be utilized thus necessitating the use of Stereolithography (SLA) additive manufacturing technique. Based on the SLA technology, the 3D printer of Form2 (FormLabs) has 50 μm special resolution scale. Its main operation principle lies in the SLA printing technology to create 3D models which utilizes a light source of ultraviolet (UV) laser or projector to selectively cure liquid resin into hardened plastic layer by layer. In this printing, the employed clear resin is featured with a permittivity of 2.8 and loss tangent of 0.03. The printing size of microfluidic channel radius, wall thickness and hemi-sphere radius are chosen as 1 mm, 0.4 mm and 8.8 mm. For the post-curing process, the printed module is firstly rinsed in isopropyl Alcohol (IPA) for 15 minutes to remove uncured resin. A post-cure chamber finalizes the polymerization process and stabilizes the mechanical properties. The clear module is required to cure at 60ºc for 15 minutes. The whole fabrication process including 3D printing, IPA washing and post curing is low-cost and fast.

B. Microfluidic Liquid Injection, Flow and Control

EGaIn (Sigma-Aldrich, 495425) is a LM alloy consisted with 75% wt Gallium and 25% wt Indium featuring 15.5ºc melting point and 29.4×10^{-6} Ω·cm resistivity. Due to its high bulk viscosity (with 1.991 mPa·s), EGaIn can flow easily in the microfluidic channel. In order to avoid the oxidation of the EGaIn, sodium hydroxide (NaOH) solution is used to restore the recycled liquid [6]. In order to stably and evenly inject, a syringe and a guiding tube stretching into the feeding channel compose the injection platform shown in Fig. 4.

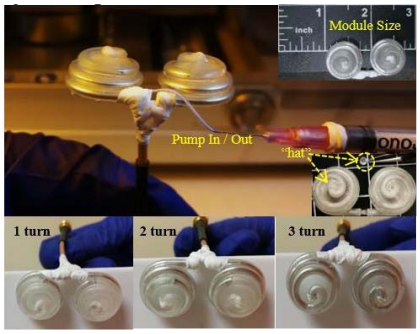

Fig. 4. The picture of the printed module, injection process and three perfectly injected static states.

For practical applications, the module can be installed inside the container of the monitored liquid. After the drug is infused to cover the module, the "hat" (a 1mm radius cylinder in the same size of the retained slot) installed to keep stable volume of the LM is removed. Once the drug level is low, the air and drug come into the channel and the monitoring function is activated. Note that the outflowed LM should be collected with another embedded container in the drug which can isolate the LM flow into the drug and permeate the monitored drug. The level of the LM decreases simultaneously with the level of the drug using communicating principle.

For experimental verifications of the monitoring function, the proposed module was initially filled up completely with LM firstly and then the LM is pumped out at 2 turns state and 1 turn state as given in Fig. 4. Used for static measurement, two extra 3D printing "hat" are stuffed into the top slots to stabilize the LM and prevent the leakage. After each injection or release of the LM, the syringe pump connected with the bottom outlet is used to collect the outflowed LM.

In order to avoid the filled LM having bubbles, the volume is calculated and quantified first and then a 1 mL syringe with scales are used to extract the LM and to inject it into the guiding tube in one-time operation. In addition, the monitoring accuracy will be influenced when air trapped between LM and drug. The "hat" should be maintained until the module is completely covered in the monitored drug.

C. Experimental Setup

In order to test at different operation situation, an Anritsu vector network analyser (VNA) is used to measure the S parameters. For radiation pattern measurement, the designed antenna was fixed at a rotation station, which can rotate 15 degrees per times. A horn antenna as a transmitter is fixed at a distance of 85 cm from the fabricated module.

D. Measurement Results

1) EGaIn at Full-state

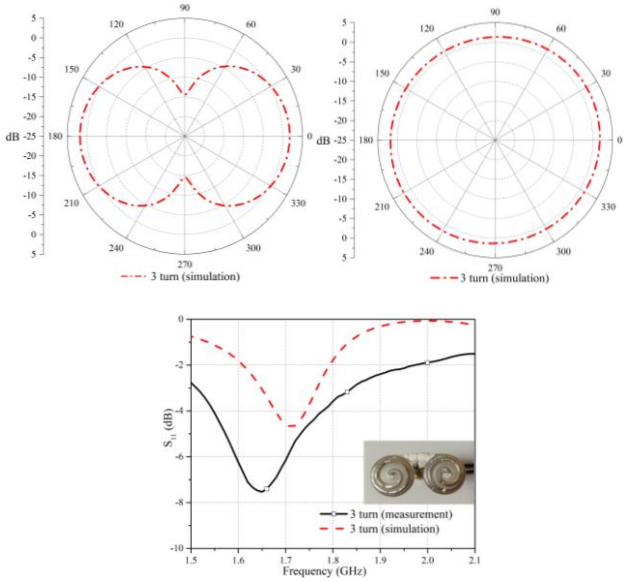

Fig. 5. The measured and simulated results of the designed module at 3-turns state.

At 3-turns injection state, the volume of the LM inside the module is 0.82 mL. Due to the limit of measurement equipment, only simulated radiation performances are given

for this state. The simulated resonant frequency is 1.71 GHz with the return loss S_{11} of -4.7 dB. The impedance matching and radiation performance of the antenna is shown in Fig. 5. The measured resonant frequency is 1.65 GHz with the S_{11} of -7.5 dB.

2) EGaIn at 2-turns State

Using the scaled syringe to control the volume of 2 turns state as 0.35 mL for each semispherical helical branch. The simulated resonant frequency is 1.96 GHz with the return loss S_{11} of -7.1 dB. The measurement results are consistent with the simulation as shown in Fig. 6. The measured resonant frequency is 2.01 GHz with the return loss S_{11} of -16.2 dB.

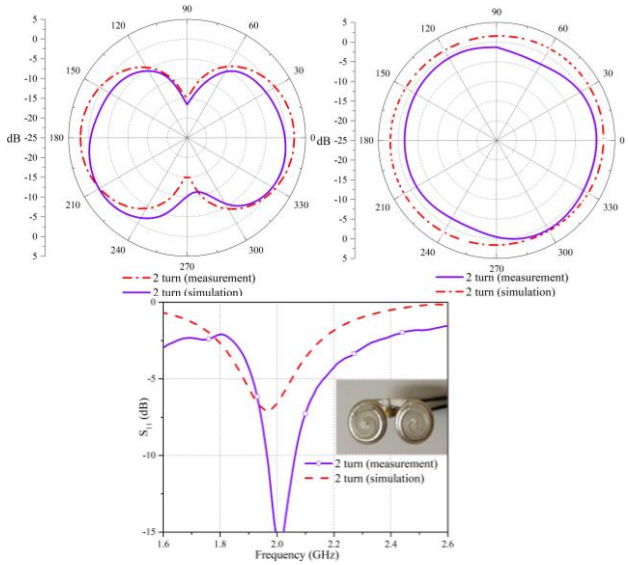

Fig. 6. The measured and simulated results of the designed module at 2-turns state.

3) EGaIn at 1-turn State

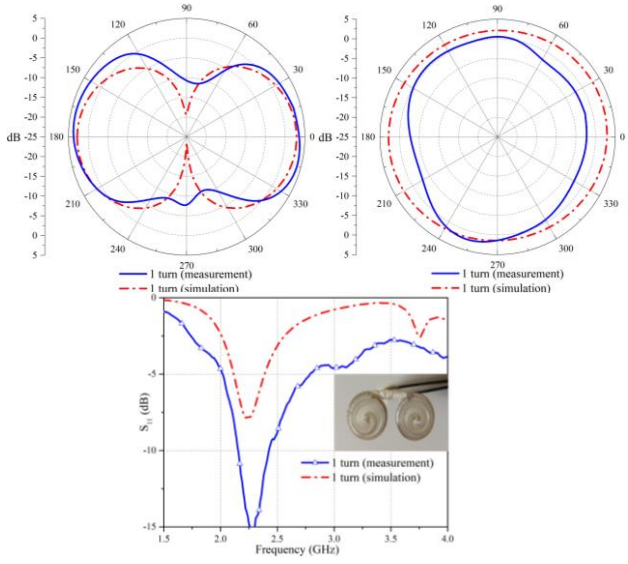

Fig. 7. The measured and simulated results of the designed module at 1-turn state.

As shown in Fig. 7, the simulated resonant frequency is 2.24 GHz with the return loss S_{11} of -8.0 dB. The measured resonant frequency is 2.28 GHz with the return loss S_{11} of -15.5 dB. Therefore, the resonant frequency shifts up along with the dosage of the LM decreases. The reason is that the lengths of the radiation arm decrease as the LM flowing out of the microfluidic channels. In this way, the volume of the contained LM can be monitored by tracking different resonant frequencies. And the level simultaneously decreases both for the LM and the monitored drug due to the communicating principle. Thus, this proposed module integrated with microfluidic design is suitable for the application of drug delivery.

IV. Conclusion

This paper proposed a spherical helix module with simple design, flexible and effective 3D printing technique and tunable microfluidic technology. The novel module owns the correlation of the resonant frequency shift with the volume of the contained liquid. These interesting features enable the functionality of the module for drug level monitoring. In addition, extension designs for various applications including chemicals storage and fuel transportation can be expected. For future design of drug monitoring application, the proposed microfluidic helix module can be improved by loading with additional dielectric liquid such as the common drugs of saline and 5% glucose solution with well-known reference resonant frequency values.

Acknowledgment

Authors would like to thank members from Agile Technologies for High-performance Electromagnetic Novel Applications at the University of Georgia Institute of Technology at Atlanta for supporting this work. This work has been supported in part by the Chinese Scholarship Council (CSC) and BUPT Excellent Ph.D. Students Foundation (No. CX2019303).

References

[1] B. Preložnik, D. Gleich, and D. Donlagic, "All-fiber, thermo-optic liquid level sensor," *Optics express*, vol. 26, pp. 23518-23533, Sep. 2018.

[2] C. Teng, et al, "Liquid level sensor based on a V-groove structure plastic optical fiber," *Sensors*, vol. 18, pp. 3111, Sep. 2018.

[3] H. Huang, et al, "RFID tag helix antenna sensors for wireless drug dosage monitoring," *IEEE J. Transl. Eng. Health Med*, vol. 2, Mar. 2014.

[4] S. A. Nauroze, et al, "Additively manufactured RF components and modules: toward empowering the birth of cost-efficient dense and ubiquitous IOT implementations," *Proceedings of the IEEE*, vol. 105, pp. 702-722, Feb. 2017.

[5] M. J. Kim, C. S. Cho, and J. Kim, "A dual band printed dipole antenna with spiral structure for WLAN application," *IEEE Microwave and Wireless Components Letters*, vol. 15, pp. 910-912, Dec. 2015.

[6] W. Su, S. A. Nauroze, B. Ryan, and M. M. Tentzeris, "Novel 3D printed liquid-metal-alloy microfluidics-based zigzag and helical antennas for origami reconfigurable antenna "trees"," in *2017 IEEE MTT-S International Microwave Symposium (IMS2017)*, IEEE, 2017, pp. 1579-1582.